Electronic Supplementary Material (ESI) for Physical Chemistry Chemical Physics.

Ultrafast dynamics of the ESIPT photoswitch N-(3-pyridinyl)-2-pyridinecarboxamide

Electronic Supplementary Information (ESI)

Hendrik Böhnke,[a,b] Julia Bahrenburg,[a,b] Xiaonan Ma,[a,c] Katharina Röttger,[a,d] Christian Näther,[e] Michał F. Rode,[f] Andrzej L. Sobolewski[f] and Friedrich Temps*[a]

Contents

---

[a] *Institute of Physical Chemistry, Christian-Albrechts-University Kiel, Olshausenstr. 40, 24098 Kiel, Germany. Fax: +49 (0)431 880 7802; Tel: +49 (0)431 880 7800; E-mail: temps@phc.uni-kiel.de*

[b] *Both authors contributed equally to this work.*

[c] *Present address: Institute of Physical and Theoretical Chemistry, Julius-Maximilians-University Würzburg, Am Hubland, 97074 Würzburg, Germany.*

[d] *Present address: Centre for Process Innovation, Wilton Centre, Wilton, Redcar TS10 4RF, United Kingdom.*

[e] *Institute of Inorganic Chemistry, Christian-Albrechts-University Kiel, Olshausenstr. 40, 24098 Kiel, Germany.*

[f] *Institute of Physics, Polish Academy of Science, al. Lotników 32/46, 02-668 Warsaw, Poland.*

1 Crystal structure data

Crystal structure determination was carried out using an Imaging Plate Diffraction System (IPDS-2) from STOE & CIE. The structure was solved using SHELXS-97 and refined against F^2 using SHELXL-2014. All non-hydrogen atoms were refined anisotropic. The C–H and N-H H atoms were located in a different map but were positioned with idealized geometry and refined isotropy with $U_{iso}(H) = 1.2\ U_{eq}(C)$ using a riding model. An ORTEP plot of NPPCA with labeling and displacement ellipsoids is given in Fig. S 1. Selected crystal data and details of the refinement can be found in Table S 1, selected bond lengths and angles are given in Table S 2 and hydrogen bonds in the crystal structure are presented in Table S 3.

CCDC 1556507 contains the supplementary crystallographic data for this paper. These data can be obtained free of charge from the Cambridge Crystallographic Data Centre via http://www.ccdc.cam.ac.uk/data_request/cif.

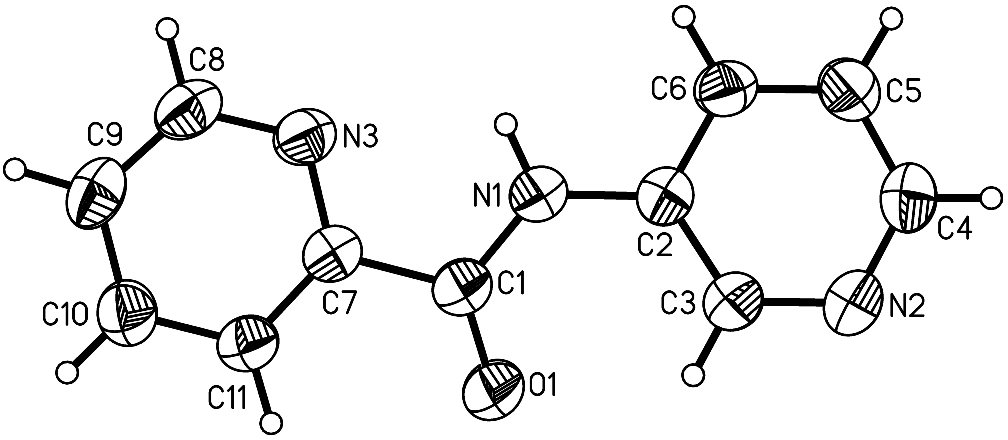

Fig. S 1: ORTEP plot of NPPCA with labeling and displacement ellipsoids drawn at the 50 % probability level indicating a pre-orientation due to intramolecular N–H···N hydrogen bonding (C2–N1–C1–C7: 178.8(2)°; dihedral angle between the 6-membered rings: 6.24(1)°; H1···N3: 2.27 Å, N1–H1···N3: 110.4°).

Table S 1: Crystal data and structure refinement parameters for NPPCA.

Empirical formula	$C_{11}H_9N_3O$
Formula weight	199.21 g/mol
Temperature	293(2) K
Wavelength	0.71073 Å
Crystal system	Monoclinic
Space group	$P2_1/n$
Unit cell dimensions	a = 5.7147(4) Å, α = 90°
	b = 8.3019(6) Å, β = 94.120(5)°
	c = 20.1261(14) Å, γ = 90°
Volume	952.37(12) $Å^3$
Z	4
Density (calculated)	1.389 Mg/m^3
Absorption coefficient	0.094 mm^{-1}
F(000)	416
Crystal size	0.3 x 0.2 x 0.2 mm^3
Theta range for data collection	2.029 to 26.002°
Index ranges	$-6 \leq h \leq 7$, $-10 \leq k \leq 10$, $-24 \leq l \leq 24$
Reflections collected	10738
Independent reflections	1875 [R(int) = 0.0639]
Observed reflections	1508
Completeness to theta = 25.242°	99.7 %
Refinement method	Full-matrix least-squares on F^2
Data / restraints / parameters	1875 / 0 / 137
Goodness-of-fit on F^2	1.082
Final R indices [I> 2σ(I)]	R1 = 0.0456, wR2 = 0.0985
R indices (all data)	R1 = 0.0631, wR2 = 0.1058
Extinction coefficient	0.031(7)
Largest diff. peak and hole	0.130 and -0.135 e.$Å^{-3}$

Table S 2: Bond lengths and angles for NPPCA.

bond	distance / Å	bond	angle / °
C(1)-O(1)	1.227(2)	O(1)-C(1)-N(1)	124.4415)
C(1)-N(1)	1.356(2)	O(1)-C(1)-C(7)	121.08(15)
C(1)-C(7)	1.497(2)	N(1)-C(1)-C(7)	114.47(14)
N(1)-C(2)	1.407(2)	C(1)-N(1)-C(2)	127.91(14)
C(2)-C(6)	1.381(2)	C(6)-C(2)-C(3)	117.76(15)
C(2)-C(3)	1.385(2)	C(6)-C(2)-N(1)	118.52(14)
C(3)-N(2)	1.333(2)	C(3)-C(2)-N(1)	123.72(15)
N(2)-C(4)	1.328(2)	N(2)-C(3)-C(2)	123.36(17)
C(4)-C(5)	1.372(3)	C(4)-N(2)-C(3)	117.80(16)
C(5)-C(6)	1.378(2)	N(2)-C(4)-C(5)	122.99(16)
C(7)-N(3)	1.339(2)	C(4)-C(5)-C(6)	118.93(16)
C(7)-C(11)	1.373(2)	C(5)-C(6)-C(2)	119.12(16)
N(3)-C(8)	1.327(2)	N(3)-C(7)-C(11)	123.40(15)
C(8)-C(9)	1.378(3)	N(3)-C(7)-C(1)	117.75(14)
C(9)-C(10)	1.372(3)	N(3)-C(7)-C(1)	117.75(14)
C(10)-C(11)	1.375(2)	C(11)-C(7)-C(1)	118.83(14)
		C(8)-N(3)-C(7)	116.50(15)
		N(3)-C(8)-C(9)	124.16(16)
		C(10)-C(9)-C(8)	118.21(16)
		C(9)-C(10)-C(11)	118.87(17)
		C(7)-C(11)-C(10)	118.80(16)

Table S 3: Hydrogen bond lengths and angles between acceptor A and donor D in the NPPCA crystal structure.

D–H···A	d(D–H) / Å	d(H···A / Å	d(D···A)	∠(D–H–A) / °
N(1)-H(1)···N(3)	0.86	2.27	2.690(2)	110.4
C(3)-H(3)···O(1)	0.93	2.27	2.875(2)	122.1
C(6)-H(6)···O(1)#1	0.93	2.53	3.216(2)	130.7
C(9)-H(9)···N(2)#2	0.93	2.63	3.428(2)	144.5

2 Calculated ground structures for tautomers I and IV

Examination of the ground-state PEHS at the MP2/cc-pVDZ level of theory yielded four local minima next to the global minimum of **I** (trans-carboxamide) at the indicated energies:

1. trans-iminol (**IV**): 0.54 eV,
2. cis-iminol (**V**): 0.80 eV,
3. trans-carboxamide rotamer (**VI**): 0.46 eV,
4. trans-iminol rotamer (**VII**): 1.15 eV.

The calculated structures for the two tautomeric forms **I** and **IV** at the RI-MP2/aug-cc-pVDZ level of theory are displayed in Fig. S 2, the respective cartesian coordinates are listed in Tables S 4 - S 5. Structure **V** is solely accessible upon excitation of **IV**. Structures **VI** and **VII** are unfavoured due to the lack of intramolecular hydrogen bonds. Structures **II** and **III** are unstable on the ground-state PEHS. Thus, the relevant ground-state structures upon $\pi\pi^*$ excitation at λ_{pump} = 266 nm are **I** and **IV**.

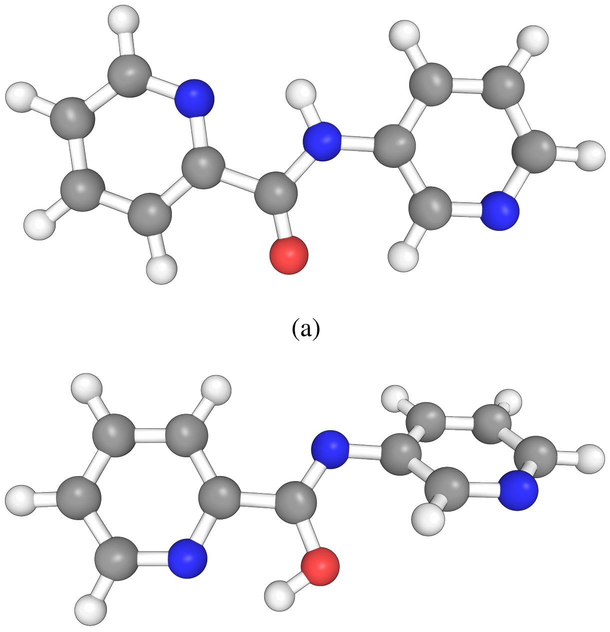

(a)

(b)

Fig. S 2: Calculated structures of NPPCA in form **I** (a) and form **IV** (b) at the RI-MP2/aug-cc-pVDZ level of theory.

Table S 4: Cartesian coordinates for the optimized structure of **I** at the RI-MP2/aug-cc-pVDZ level of theory.

atom	X / Å	Y / Å	Z / Å
C	-3.2552498	1.4074652	-0.0001088
C	-4.3779865	0.5598759	0.0001076
C	-4.1763963	-0.8318847	0.0001231
C	-2.8610469	-1.3207577	-0.0000577
C	-1.8048061	-0.3916027	-0.0001076
N	-1.9844740	0.9522004	-0.0001861
H	-5.0269817	-1.5192319	0.0003015
H	-3.3772861	2.4950371	-0.0002739
H	-5.3843110	0.9866909	0.0003071
H	-2.6276162	-2.3874744	-0.0002697
C	-0.3826230	-0.9010829	-0.0000001
O	-0.1260407	-2.1111191	0.0001056
N	0.5362934	0.1167777	-0.0000197
H	0.1094561	1.0447313	0.0000321
C	2.6693224	1.2362960	-0.0000335
C	1.9377759	0.0289066	-0.0000588
C	2.6542971	-1.1939771	-0.0000650
C	4.6913422	-0.0830269	0.0000713
H	2.1209626	-2.1438636	-0.0001448
H	2.1433616	2.1972100	-0.0001167
H	5.7826823	-0.1659935	0.0001306
N	4.0058526	-1.2466018	0.0000138
C	4.0675888	1.1781375	0.0000661
H	4.6658832	2.0932877	0.0001837

Table S 5: Cartesian coordinates for the optimized structure of **IV** at the RI-MP2/aug-cc-pVDZ level of theory.

atom	X / Å	Y / Å	Z / Å
C	-3.7409332	1.4198357	0.2731449
C	-4.5700137	0.3718899	-0.1706472
C	-3.9759963	-0.8170417	-0.6270241
C	-1.8511297	0.0139658	-0.2302467
H	-4.5883134	-1.6524992	-0.9790830
H	-4.1734214	2.3569520	0.6345498
H	-5.6585812	0.4702044	-0.1640342
C	-0.3911439	-0.2751950	-0.3012480
N	0.4629101	0.6312486	0.0478478
C	2.7101127	1.3437559	-0.5110000
C	1.8481500	0.3503541	-0.0044916
C	2.4289087	-0.8320616	0.5160451
C	4.5665938	-0.1139609	0.0181629
H	1.7911570	-1.6096873	0.9458570
H	2.2876391	2.2789586	-0.8899148
H	5.6392601	-0.3314880	0.0379583
N	3.7579978	-1.0656058	0.5394596
C	4.0907540	1.0981773	-0.5134762
H	4.7926920	1.8376262	-0.9093020
N	-2.6389003	-1.0019971	-0.6586392
C	-2.3505979	1.2417103	0.2440542
H	-1.6489803	2.0110279	0.5725796
O	-0.0809844	-1.5073746	-0.7725247
H	-0.9522796	-1.9190953	-0.9779275

3 Calculated excitation energies and UV spectra

Table S 6: Vertical excitation energies of **I**, **IV**, **V**, **VI** and **VII** at the CC2/ cc-pVDZ level of theory for MP2/cc-pVDZ optimized geometries relative to the global minimum of **I**.

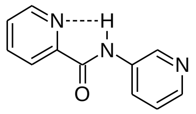				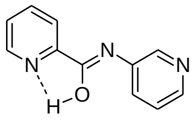				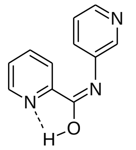			
I				**IV**				**V**			
state	ΔE/eV	f	μ/Debye	state	ΔE/eV	f	μ/Debye	state	ΔE/eV	f	μ/Debye
S_0	0.00	-	4.2	S_0	0.54	-	5.2	S_0	0.80	-	5.2
nπ^*	4.44	0.001	1.6	$\pi\pi^*$	4.45	0.745	2.1	$\pi\pi^*$	3.98	0.041	5.6
$\pi\pi^*$	4.70	0.394	3.9	nπ^*	4.62	0.002	2.4	$\pi\pi^*$	4.67	0.064	2.2
$\pi\pi^*$	4.93	0.056	3.2	$\pi\pi^*$	4.93	0.016	3.9	$\pi\pi^*$	4.84	0.124	2.8
$\pi\pi^*$	5.13	0.025	3.4	nπ^*	4.93	0.001	0.2	nπ^*	5.09	0.007	4.4
nπ^*	5.24	0.006	3.3	$\pi\pi^*$	5.11	0.054	2.1	$\pi\pi^*$	5.10	0.021	2.4
nπ^*	5.28	0.000	2.8	nπ^*	5.26	0.003	3.1		5.23	0.001	2.7
$\pi\pi^*$	5.86	0.225	10.4	$\pi\pi^*$	5.82	0.023	5.3		5.28	0.010	3.3
$\pi\pi^*$	6.30	0.214	3.2	$\pi\pi^*$	6.18	0.108	1.8	$\pi\pi^*$	5.53	0.089	2.9
$\pi\pi^*$	6.35	0.006	2.7	$\pi\pi^*$	6.43	0.062	7.4		5.65	0.006	2.6
								$\pi\pi^*$	5.86	0.147	3.9
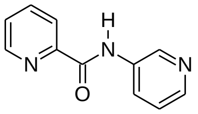				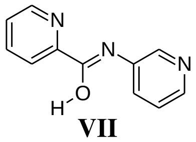							
VI				**VII**							
state	ΔE/eV	f	μ/Debye	state	ΔE/eV	f	μ/Debye				
S_0	0.46	-	3.9	S_0	1.15	-	6.6				
S_1	4.67	0.002	0.7	S_1	4.46	0.316	4.0				
S_2	4.89	0.112	4.7	S_2	4.76	0.070	4.7				
S_3	5.01	0.027	2.1	S_3	4.90	0.040	1.9				
S_4	5.13	0.134	1.2	S_4	4.99	0.009	6.2				
S_5	5.18	0.118	1.7	S_5	5.04	0.007	4.0				
S_6	5.23	0.123	3.2	S_6	5.11	0.003	3.7				
S_7	5.27	0.004	5.0								
S_8	5.54	0.002	5.5								
S_9	6.04	0.016	12.3								
S_{10}	6.14	0.042	9.3								

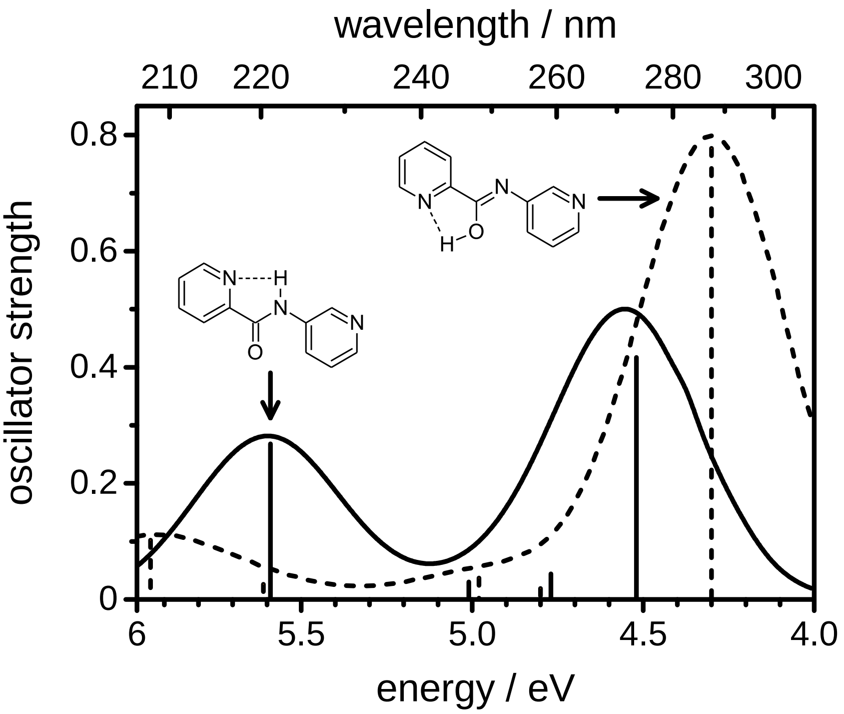

Fig. S 3: Calculated UV/VIS spectra of NPPCA in forms **I** (solid black line) and **IV** (dashed black line) at the CC2/aug-cc-pVDZ level of theory.

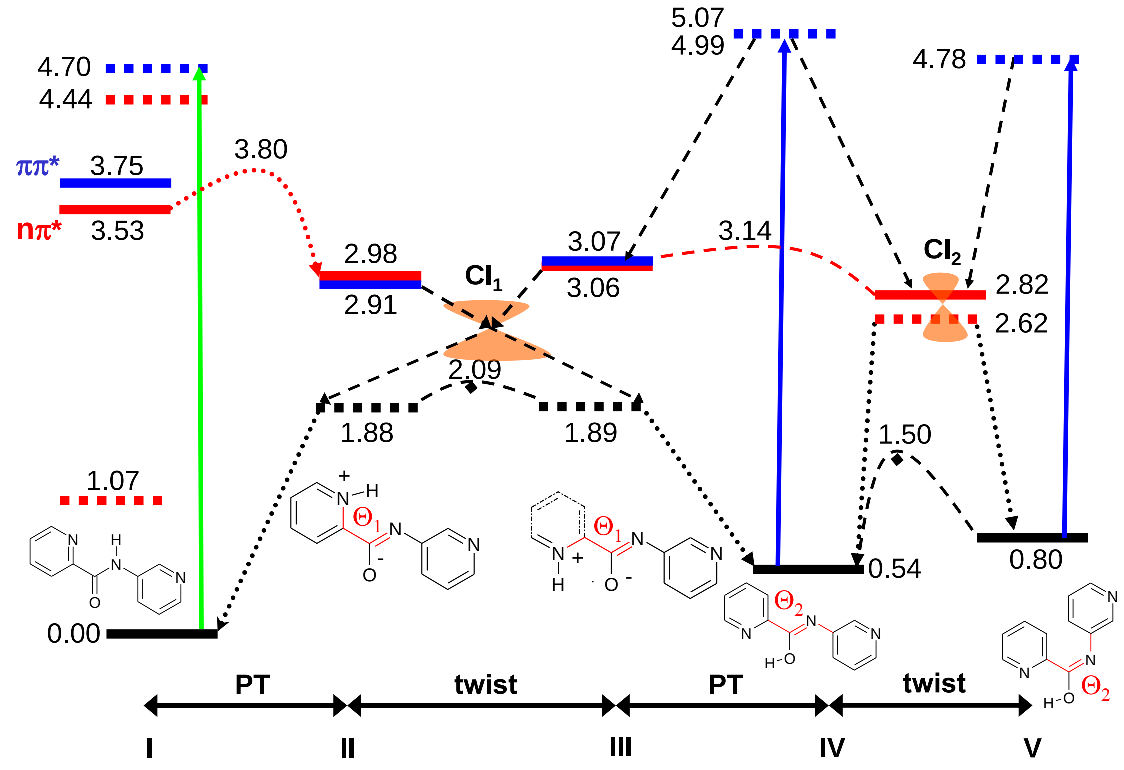

Fig. S 4: Computational results pertaining to the ground-state and excited-state potential energy surfaces for NPPCA.

4 Time profiles and decay time constants for NPPCA in water

TEAS measurements for NPPCA in water, where all hydrogen bonding sites are occupied by H_2O molecules so that intramolecular proton transfer to **IV** is unlikely, showed fast transient absorption decays without long-lived 20 ps lifetime components. A comparison of measured transient absorption–time profiles in ACN and H_2O at two probe wavelengths is shown in Fig. S 5.

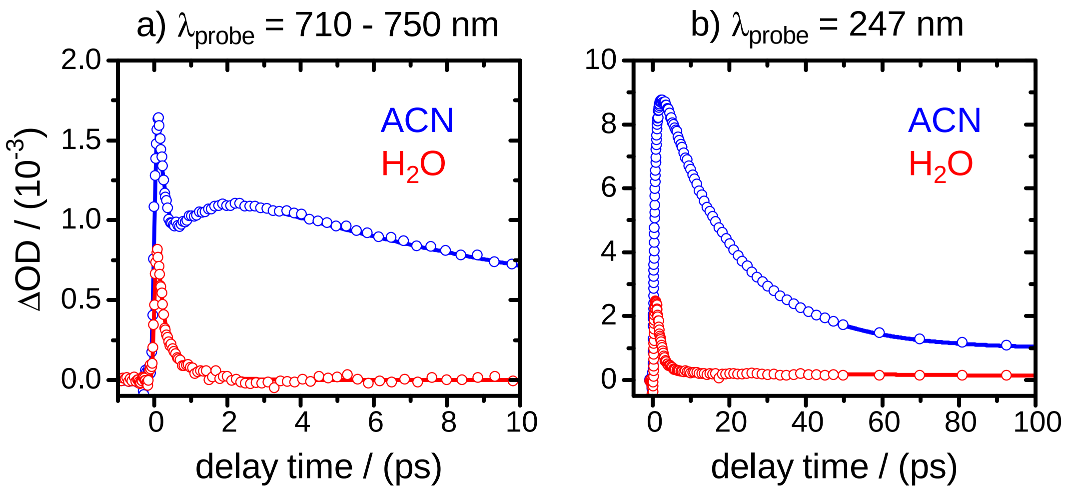

Fig. S 5: Comparison of the transient absorption-time profiles of NPPCA in ACN (blue) and H_2O (red) at a) λ_{probe} = 710 – 750 nm and b) λ_{probe} = 247 nm after photoexcitation at λ_{pump} = 264 nm. The measurements in ACN and H_2O were made directly one after the other, so that a direct comparison of the data is possible.

Figure S 6 shows a set of absorption and fluorescence decay time profiles for NPPCA in H_2O after integration over the distinct transient absorption bands in the spectro-temporal absorption map of Fig. 3d. A simultaneous least-squares fit to the absorption data yielded the following three time constant values:

$$\tau_1 = 0.08 \pm 0.01 \text{ ps},$$
$$\tau_2 = 0.30 \pm 0.02 \text{ ps},$$
$$\tau_3 = 1.32 \pm 0.05 \text{ ps}.$$

The fluorescence decay time profiles were found to be described by

$$\tau_{1,\mathrm{TFL}} = 0.15 \pm 0.02 \text{ ps},$$
$$\tau_{2,\mathrm{TFL}} = 0.46 \pm 0.05 \text{ ps}.$$

The results were confirmed by singular value decomposition (SVD) analysis. The obtained decay-associated spectra and SVD time profiles are displayed in Fig. S 7 (H_2O) and Fig. S 8 (ACN).

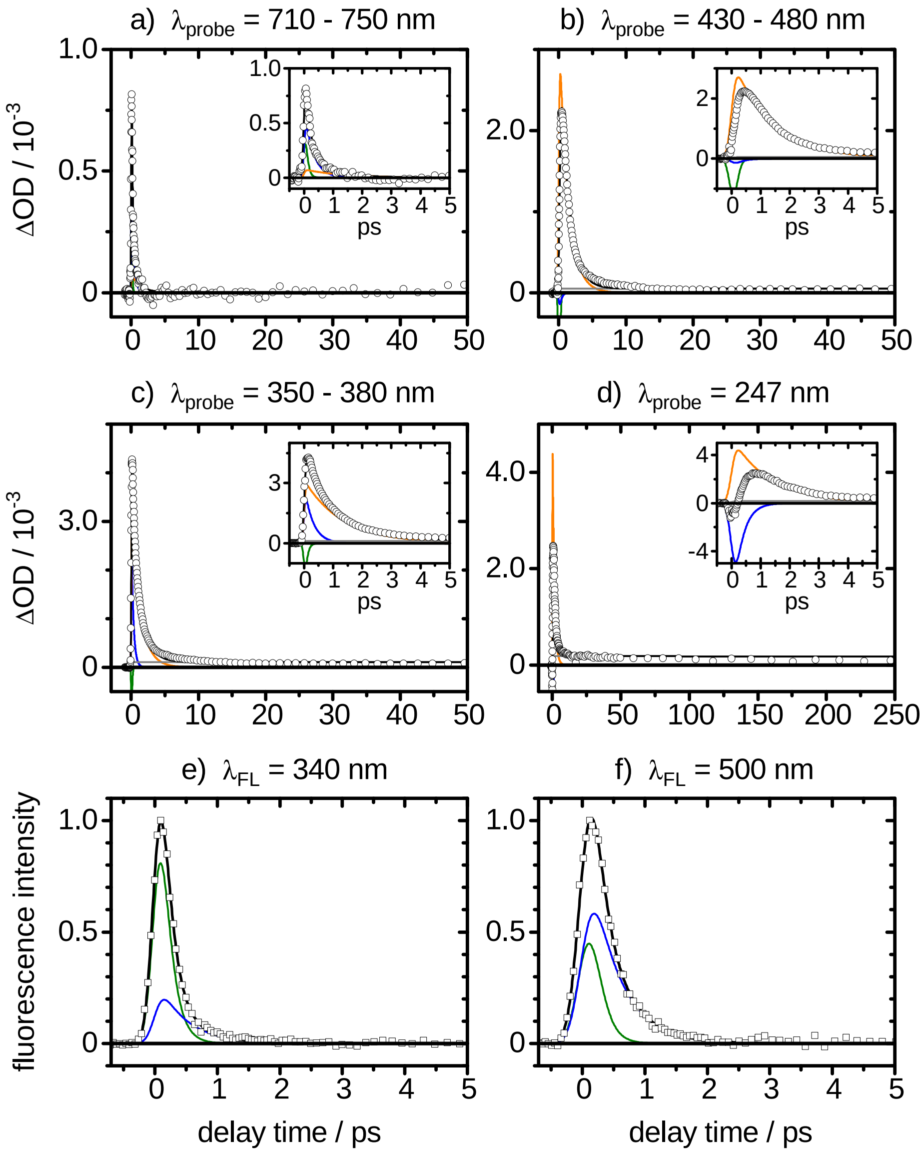

Fig. S 6: a - d) Transient absorption–time profiles of NPPCA in H_2O after excitation at λ_{pump} = 264 nm in four selected probe windows (a: 710 – 750 nm, b: 430 – 480 nm, c: 350 – 380 nm, d: 247 nm). e - f) Fluorescence–time profiles of NPPCA in H_2O after excitation at λ_{pump} = 264 nm at two emission wavelengths (e: λ_{FL} = 340 nm, f: λ_{FL} = 500 nm).

5 SVD analysis of the transient absorption matrix for NPPCA in water

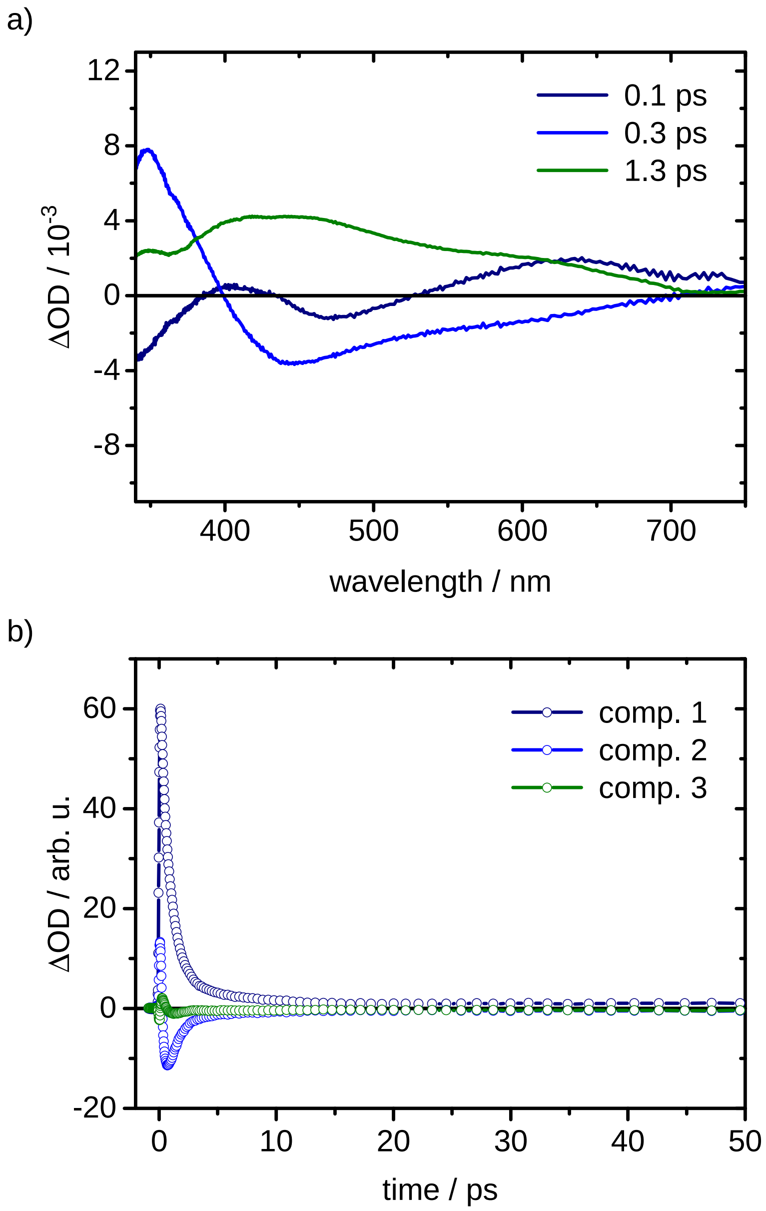

Fig. S 7: a) Decay-associated spectra and b) SVD time profiles for NPPCA in H_2O.

6 SVD analysis of the transient absorption matrix for NPPCA in ACN

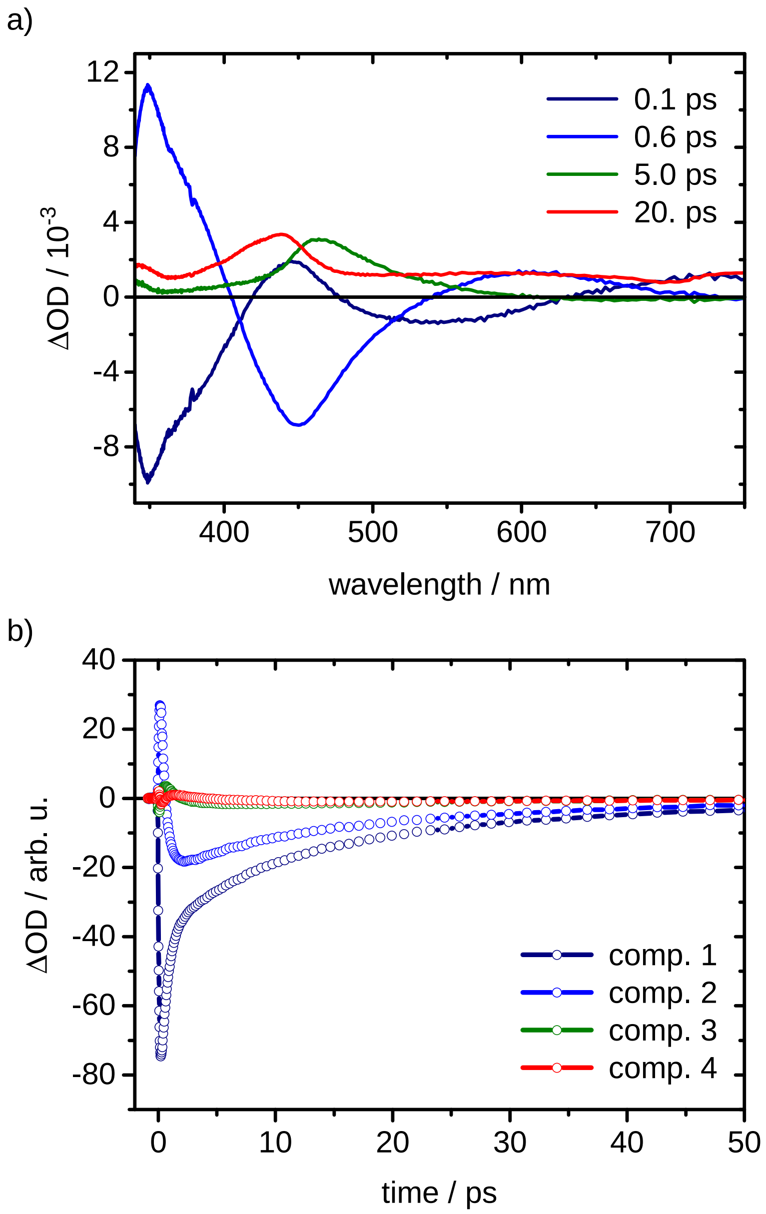

Fig. S 8: a) Decay-associated spectra and b) SVD time profiles for NPPCA in ACN.

7 Comparison of experimental and calculated vibrational spectra

FTIR spectra were recorded at a nominal resolution of 1 cm^{-1} on a Bruker IFS66v spectrometer equipped with a with liquid nitrogen-cooled MCT detector. The sample compartment was continuously purged with dry air containing < 1 ppm water vapour and < 1 ppm CO_2. The CaF_2 cell had an optical path length of 100 μm to allow for measurements from 600 – 5000 cm^{-1}.

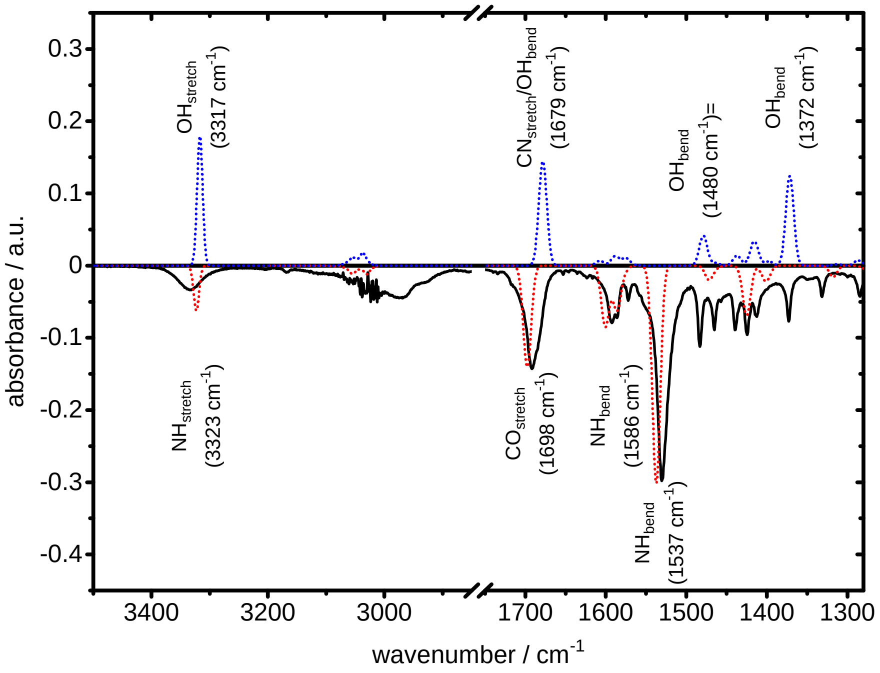

Fig. S 9: FTIR spectrum of NPPCA (**I**) in $CHCl_3$ (negative solid black line) compared with calculated RI-MP2/aug-cc-pVDZ vibrational spectra for **I** (negative dotted red line) and **IV** (positive dotted blue line) using scaling factors of 0.985 below 1800 cm^{-1} and 0.945 above 1800 cm^{-1}. The respective vibrational modes are illustrated in Fig. S 10.

structure **I** structure **IV**

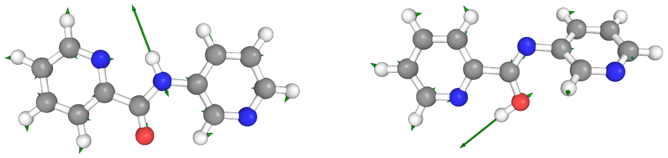

a) $\nu(\mathrm{NH_{stretch}})$ 3323 cm^{-1}

e) $\nu(\mathrm{OH_{stretch}})$ 3317 cm^{-1}

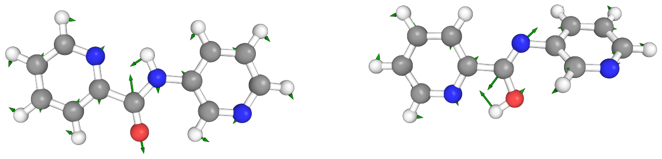

b) $\nu(\mathrm{CO_{stretch}})$ 1698 cm^{-1}

f) $\nu(\mathrm{CN_{stretch}})/\mathrm{OH_{bend}})$ 1679 cm^{-1}

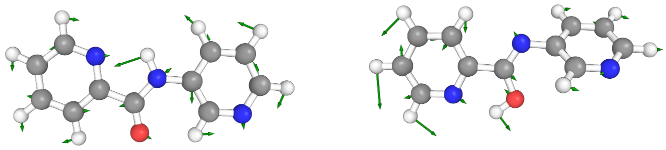

c) $\nu(\mathrm{NH_{bend}})$ 1586 cm^{-1}

g) $\nu(\mathrm{OH_{bend}}/\mathrm{CH_{bend}})$ 1480 cm^{-1}

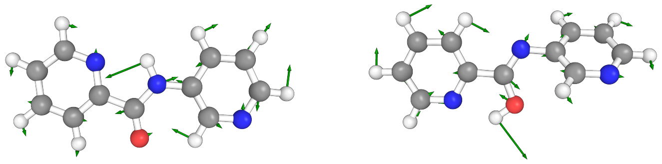

d) $\nu(\mathrm{NH_{bend}})$ 1537 cm^{-1}

h) $\nu(\mathrm{OH_{bend}})$ 1372 cm^{-1}

Fig. S 10: Vibrational marker modes of the electronic ground state species **I** and **IV** calculated at the RI-MP2/aug-cc-pVDZ level of theory. Wavenumbers are given after applying scaling factors of 0.985 below 1800 cm^{-1} and 0.945 above 1800 cm^{-1}.

8 Comparison of a late-time TVA spectrum to calculated vibrational spectra for structures I and IV

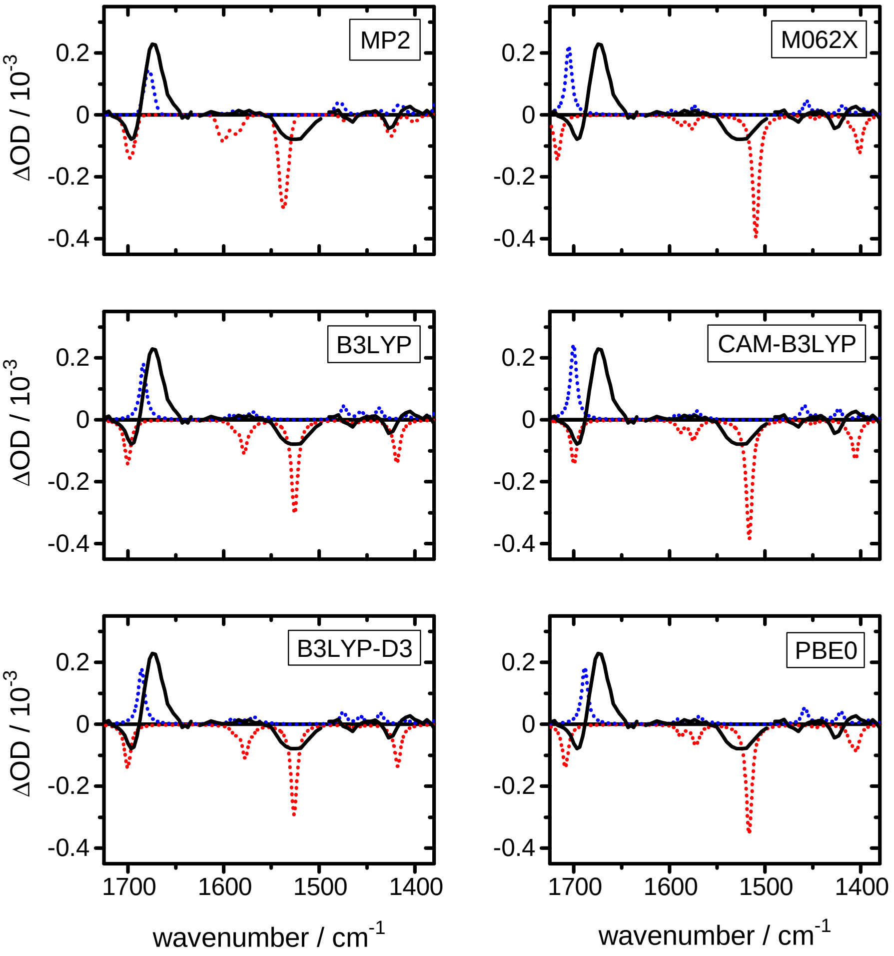

Fig. S 11: Comparison of the measured TVA spectrum at Δt = 850 ps (black solid lines) with calculations for **I** shown in the negative direction (red dotted lines) and for **IV** shown in the positive direction (blue dotted lines). The calculations were performed at the RI-MP2/aug-cc-pVDZ, B3LYP/6-311+G**, B3LYP-D3/6-311+G**, M062X/6-311+G**, CAM-B3LYP/6-311+G** and PBE0/6-311+G** levels of theory using scaling factors of 0.985, 0.975, 0.975, 0.95, 0.95 and 0.955, respectively.